Silver-doped silver vanadate glass composite electrolyte: structure and an investigation of electrical properties

Emad M. Masoud & M. A. Mousa

Ionics
International Journal of Ionics The Science and Technology of Ionic Motion

ISSN 0947-7047
Volume 21
Number 4

Ionics (2015) 21:1095-1103
DOI 10.1007/s11581-014-1283-0

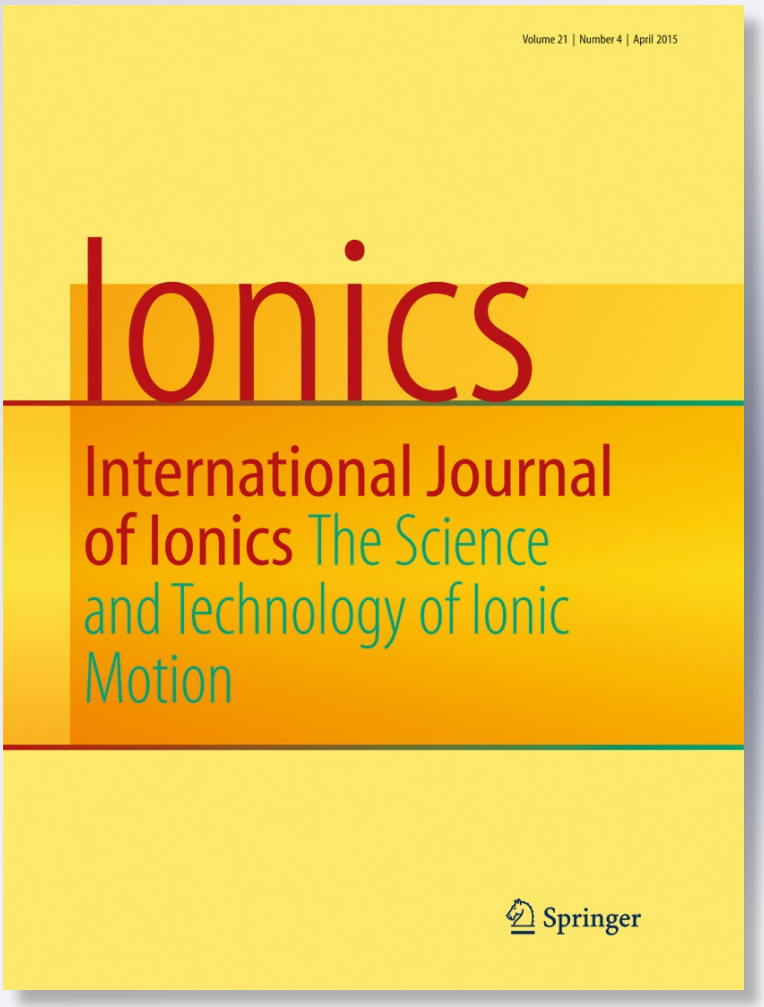

Springer

Ionics (2015) 21:1095–1103
DOI 10.1007/s11581-014-1283-0

ORIGINAL PAPER

Silver-doped silver vanadate glass composite electrolyte: structure and an investigation of electrical properties

Emad M. Masoud · M. A. Mousa

Received: 19 June 2014 / Revised: 6 September 2014 / Accepted: 5 October 2014 / Published online: 29 October 2014

Abstract Structural and electrical properties of the ternary ionic–electronic conducting glass system xAgI–(1−x)[0.67Ag_2O–0.33V_2O_5], where x=0.4, 0.5, 0.6, 0.7, and 0.8 were studied for emphasizing the influence of silver iodide concentration on the transport properties of the based vanadate glasses. The glasses were prepared by melt quenching technique and characterized using X-ray diffraction (XRD), FTIR spectra, and differential thermal analysis (DTA). Electrical conductivity (σ), dielectric constant (ε′), dielectric loss (ε″), and impedance spectra (Z'-Z'') were studied for all samples. All glasses showed a mixed ionic–electronic conductance with a high ionic conductivity for the sample with x=0.7. The electronic contribution to the total conductivity and the ionic (t_i) and electronic transport numbers (t_e) were determined for each glass sample using Wagner's DC polarization technique. The variation in electrical properties with each of composition, temperature, and frequency was analyzed and discussed.

Keywords Amorphous materials · Glasses · Electrical properties

Introduction

Electrical properties of glasses have been studied extensively for a number of years due to their potential use in solid-state devices. Electrical conduction in glasses occurs through different mechanisms as ionic, electronic, or mixed type. The ionic conduction is found to be predominated in AgI-based glasses [1–4]. These glasses are the most widely ionic conducting materials received more attention for their different applications. However, the addition of transition metal oxide makes them electronic or mixed electronic–ionic conductors, which are of potential interest as cathode materials for solid-state battery [5–9]. In order to understand the conduction mechanism in these glasses, it is essential to know their structural properties and the environment around the mobile ion. The present work was designed to study the influence of AgI concentration upon the electrical conduction properties of the system, xAgI–(1−x)[0.67Ag_2O–0.33V_2O_5], where x=0.4, 0.5, 0.6, 0.7, and 0.8. In this system, V_2O_5 works as a glass network, Ag_2O as a modifier, and AgI as a dopant responsible for high Ag^+ conductivity.

Experimental

Reagent grades AgI, Ag_2O, and V_2O_5 were used to prepare glass samples with a general formula of xAgI–(1−x)[0.67Ag_2O–0.33V_2O_5], where x=0.4, 0.5, 0.6, 0.7, and 0.8, using melt quenching technique. The appropriate amounts were mixed together and ground to obtain homogeneous mixtures. The mixtures were then melted at 1,223 K in a porcelain crucible for 30 min. The homogeneous melt was rapidly quenched onto a stainless steel plate maintained at room temperature.

The prepared samples were characterized by X-ray diffraction method using a Phillips X-ray diffractometer (Model PW 1710). Density of the glasses was measured by Archimedes's

E. M. Masoud (✉) · M. A. Mousa
Chemistry Department, Faculty of Science, Benha University, 13518 Benha, Egypt
e-mail: emad_masoud1981@yahoo.com

method using toluene as an immersion liquid. The thermal stability of the samples was studied in a static air atmosphere at a constant heating rate of 10 K/min over a temperature range of 303–603 K using Shimadzu DT-40. Fourier transform infrared (FTIR) spectra were recorded using KBr pellet on IR-Bruker, Vector 22, Germany.

For electrical measurements, the quenched samples prepared as rectangular plates were polished using SiC paper up to 1,200 grit. Aluminum was evaporated onto opposite sides to form electrodes for conductivity experiment. Linear *I–V* characteristics confirmed that electrodes provide an ohmic (non-Schottky type) contact for electronic conduction. Typical thickness and area of the samples were in the range of 0.7–1.5 mm and 6–8 mm^2, respectively. Samples of 5 mm were also prepared to investigate the effect of contact resistance on the conductivity results for glasses with high conductivity, and the difference was found to be negligible. Electrical properties were obtained by measuring complex impedance using a programmable automatic LCR bridge (model RM 6306 Phillips Bridge) over a frequency range from 10^2 Hz to 1 MHz and in a temperature range from 303 to 413 K. The dc electrical measurement was carried out by means of the four-point method [10] using a Keithley 487 picoamperemeter.

Results and discussion

Figure 1 shows X-ray diffraction (XRD) spectra for xAgI–$(1-x)$[$0.67Ag_2O$–$0.33V_2O_5$] samples, where x=0.4, 0.5, 0.6, 0.7, and 0.8. The figure shows amorphous structure for all compositions; except sample with x=0.8 that showed amorphous structure with some peaks characteristic to α- and β-AgI crystals [11] present in the sample. This may be attributed to the limited solubility of AgI in this glass matrix.

The FTIR spectra of the studied glasses are shown in Fig. 2. The spectra exhibit marked absorption bands at about 498, 665, 891, 919, and 961 cm^{-1} for all samples. The bands at 891, 919, and 961 cm^{-1} correspond to the VO_3 terminal stretching of pyrovanadate ions, and 498 cm^{-1} correspond to V–O–V anti-symmetric stretching modes [12]. For all samples, a transmission band at 690 cm^{-1} was observed. This is assigned to VO_4^{3-} stretching mode. Dimitriev et al. [13] reported that the band at ~1,000 cm^{-1} in Ag_2O–V_2O_5 glassy system is due to bonding of Ag^+ ions with the unbridged double-bonded oxygen.

The band appearing at 665 cm^{-1} is attributed to the symmetric V–O–V vibrations [14]. The characteristic vibrational bands for the isolated vanadium–oxygen bonds are appearing in the range 536–560 cm^{-1} [15]. This is attributed to the vibrations of VO_2 groups of the VO_4^{3-} polyhedral [14].

Generally, the IR results indicated the formation of $V_2O_7^{4-}$ and VO_4^{3-} groups in these compounds and the presence of interaction between Ag^+ ions and the non-bridging oxygen. More analysis for IR spectra shows that IR band positions are changing with AgI content in the vanadate glasses. This suggests that vanadate glass network is changing with the AgI content, referring to that the glass is composed of ionic clusters of vanadate, silver, and iodine.

Figure 3 shows differential thermal analysis (DTA) thermograms of the investigated samples. For each sample, a glass transition temperature (T_g) was observed and followed by an endothermic peak due to melting of the sample. The glass transition temperature (T_g) was found to decrease with AgI

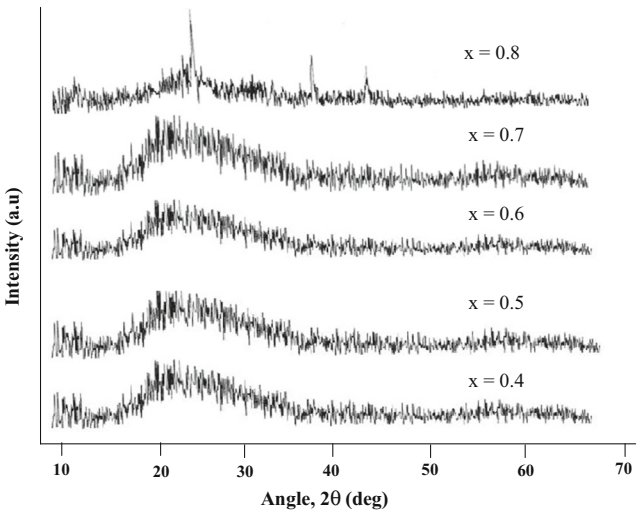

Fig. 1 XRD for xAgI–$(1-x)$[$0.67Ag_2O$–$0.33V_2O_5$] glasses, where x= 0.4, 0.5, 0.6, 0.7, and 0.8

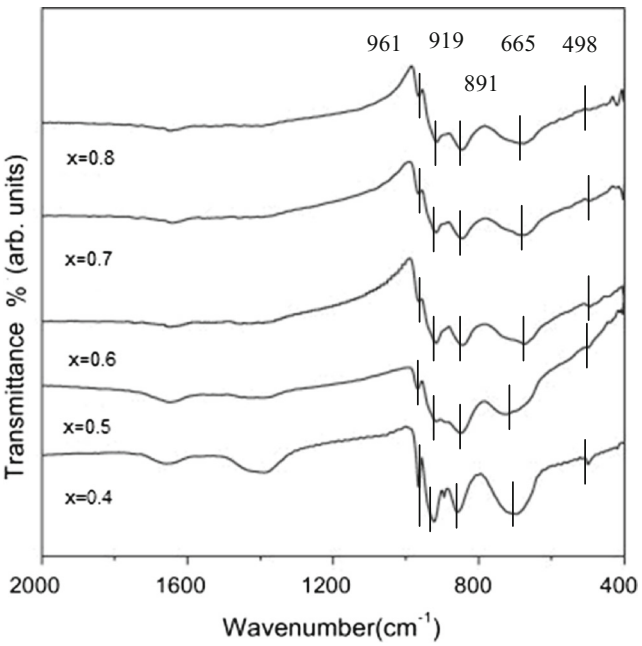

Fig. 2 FTIR for xAgI–$(1-x)$[$0.67Ag_2O$–$0.33V_2O_5$] glasses, where x= 0.4, 0.5, 0.6, 0.7, and 0.8

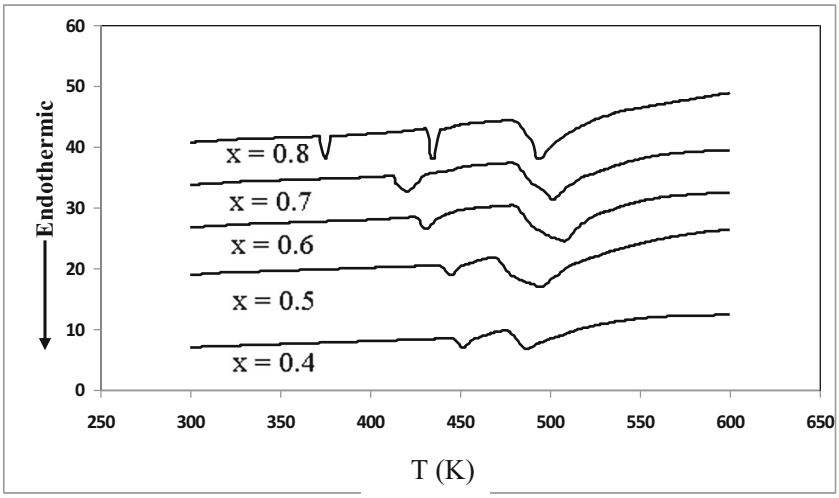

Fig. 3 DTA for xAgI–(1−x)[0.67Ag_2O–0.33V_2O_5] glasses, where x=0.4, 0.5, 0.6, 0.7, and 0.8

content increase in the glass, except for the sample with x=0.8 that showed also an endothermic peak at 375 K, due to $\beta \rightarrow \alpha$ phase transition of AgI [11]. The glass transition is a measure of strength of the glass, and the decrease in T_g with AgI content increase suggests that a larger number of bonds are destroyed within the glassy network, in order to allow its rearrangement to form a more open type with thermodynamically stable phase [11]. The thermal data are listed in Table 1.

The glass density decreases with AgI increase up to x=0.7 before starting to increase again at x=0.8 (Table 1). The density decrease can be attributed to the formation of more opened network structure with AgI content increasing in the sample due to destruction of bonds in the glass network. The abnormal behavior for sample with x=0.8 may be attributed to the presence of some crystallites of AgI confirmed by XRD results.

The complex impedance analysis method was used to test the effect of glass composition on the type of conduction. Figure 4 represents impedance/admittance spectra for samples with different compositions at 303 K. The spectra of the glasses show semicircular arcs attributable to bulk and surface effects behavior. Depressed semicircles and inclined spike [16] refer to the blocking electrode behavior for all glass samples. The left-hand admittance semicircles correspond to the polarization, and the starting position of the semicircle is a direct measure of the electronic conductivity. The formation of an inclined straight line at the low-frequency region represents the capacitance effect at the electrode and electrolyte interfaces, and this is called the double-layer capacitance effect. The corresponding equivalent electric circuit is shown in Fig. 4: R_e and R_i are the resistances related to the electronic (e) and ionic (i) components of the total electric conductivity, and CPE_g and CPE_{dl} are constant phase elements representing the geometric and double-layer capacitance of the system, respectively.

The glasses investigated in the present study contain a vanadium transition element. Vanadium ions are expected to exist mainly in V^{5+} states in the glass matrix. However, during the melting of the glasses at higher temperatures, there is ever possibility for the following redox equilibrium to take place:

$$2V^{5+} + O^{2-} \rightarrow 2V^{4+} + \frac{1}{2}O_2\uparrow \quad (1)$$

These pairs of aliovalent vanadium ions are responsible for the electronic conduction in our system. Therefore, it is expected that the electronic transfer in the investigated glasses occurred by electron hopping along $V^{4+} \rightarrow O \rightarrow V^{5+}$ bonds [17]. This electronic part was determined quantitatively by a transport number measurement through Wagner polarization technique. In this technique, the same samples used in impedance spectroscopy were also used for this purpose with sputtered gold electrodes blocking for the Ag^+ ions. On application of DC voltage (100 mV) to this configuration, an instantaneous initial current, I_0, is produced. After a long interval of 48 h, the cell is completely polarized and delivers a steady current, I_s. A decrease in the polarization

Table 1 Density Molar volume and thermal analyses data for the glass system xAgI–(1−x)[0.67Ag_2O–0.33V_2O_5] (x=0.4, 0.5, 0.6, 0.7, and 0.8

xAgI	Phase transition (K)	T_g (K)	T_m (K)	Density (g/cm^3)	Molar volume (cm^3/mol)
0.4	–	452	487	5.92	31.2
0.5	–	444	495	5.82	33.5
0.6	–	431	509	5.73	35.4
0.7	–	420	502	5.65	37.1
0.8	375	435	494	6.33	34.5

T_g glass transition temperature, T_m melting point

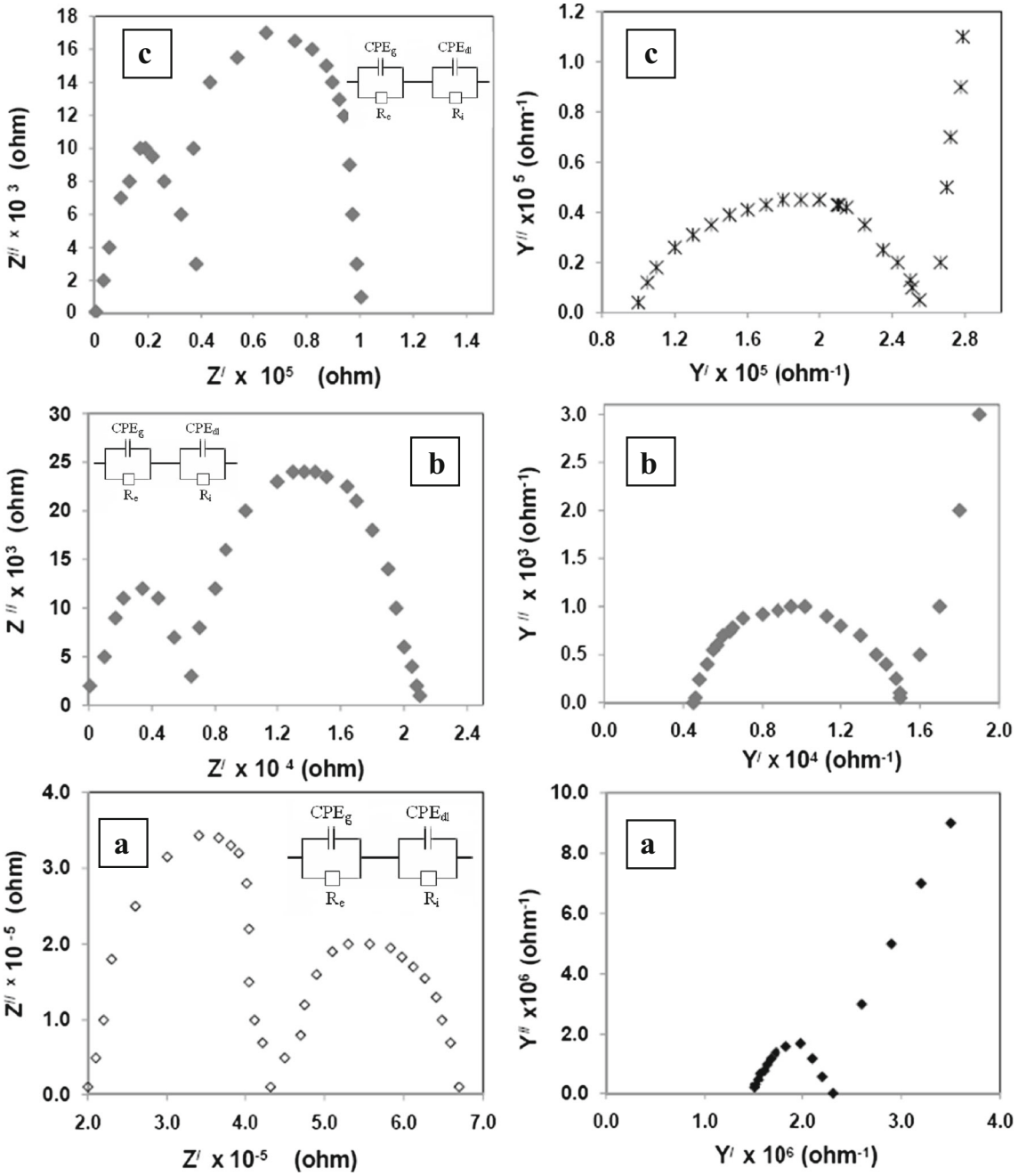

Fig. 4 Impedance (Z) and admittance (Y) spectra at 303 K for glassy samples with x=0.4 (**a**), x=0.6 (**b**), and x=0.8 (**c**)

current is attributed to migration of ions due to applied field and is balanced by diffusion due to concentration gradient. The ionic contribution is evaluated through the following equation [18]

$$t_i = 1 - I_s/I_0 \tag{2}$$

where t_i is the ionic transference number. Each of ionic conductivity (σ_i), electronic conductivity (σ_e), and ionic transfer number are calculated at room temperature and given in Table 2. From which it can be seen that the ionic conductivity increases with increasing the content of AgI in the glass matrix, except for the sample with x=0.8. This is explained according to the electrical conductivity (σ) expressed as

$$\sigma = ne\mu \tag{3}$$

where n is the number of charge carriers, e is the charge, and μ is the mobility. By increasing AgI content in the glass, the number of charge carrier (Ag^+) increases and the glass network is changed to be more open, causing an increase in the mobility of Ag^+. The decrease in ionic conductivity for the sample with x=0.8 may be attributed to the formation of AgI crystallites in the glass texture of the sample (as confirmed

Table 2 Electrical conductivity data for the glass system xAgI–$(1-x)$[$0.67Ag_2O$–$0.33V_2O_5$] (x=0.4, 0.5, 0.6, 0.7, and 0.8)

xAgI	E_{DC} (eV)	$\sigma_{DC}\times10^4$ ohm^{-1} cm^{-1}	W_m (eV)	$\sigma_i\times10^4$ ohm^{-1} cm^{-1}	$\sigma_e\times10^4$ ohm^{-1} cm^{-1}	t_i
0.4	0.58	2.3×10^{-2}	0.45	0.8×10^{-2}	1.5×10^{-2}	0.35
0.5	0.40	6.1×10^{-2}	0.35	2.9×10^{-2}	2.8×10^{-2}	0.51
0.6	0.30	1.5	0.27	1.05	0.45	0.70
0.7	0.32	4.85	0.25	3.75	1.0	0.79
0.8	3.2 (for T<380 K) 1.52 (for T>380 K)	0.27	0.49	0.16	0.1	0.61

σ_{DC}, σ_i, and σ_e are calculated at 303 K

from XRD and DTA), which may hinder the motion of Ag^+ ions in the glass matrix.

The temperature dependence of DC electrical conductivity (σ_{DC}) for the investigated system shows an Arrhenius type according to Eq. 4 (Fig. 5):

$$\sigma_{DC} = \sigma_0/T \exp.(-E_a/kT) \quad (4)$$

where σ_0 is the pre-exponential factor, E_a is the activation energy, k is the Boltzmann constant, and T is the absolute temperature. The E_a values were obtained from the linear fit of the data from Eq. 4, and the results obtained are listed in Table 2. At room temperature, σ_{DC} was found to change with the composition of the samples, according to the following order:

$$\sigma_{DC}(x=0.7) > \sigma_{DC}(x=0.6) > \sigma_{DC}\ (x=0.8) > \sigma_{DC}\ (x=0.5) > \sigma_{DC}\ (x=0.4)$$

This indicates that the conductivity increases with AgI concentration, except for the sample with x=0.8. This can be explained on the basis that AgI not only supplies mobile Ag^+ ions to the glassy samples but also facilitates their motion in the I^- lattice environment. This environment, in which stronger covalent bonding is replaced by weaker ionic one, is a decisive factor for high ionic conductivity of the best silver ion conductors like α-AgI [19]. The activation of DC conductivity (σ_{DC}) with temperature increasing can be interpreted according to Minami's structural model [20], which refers to the presence of three types of Ag^+ with different mobilities in the AgI-based ionic glasses: (i) Ag^+ ions bonded to the oxygen atoms of the network, (ii) Ag^+ ions weakly interact with the network oxygen atoms, (iii) Ag^+ ions surrounded by I^- ions only. Silver ions of the last type have a maximum mobility and contribute mostly to ionic conduction. By increasing the temperature, the conductivity increases because the Ag^+ ions (which interact weakly to the oxygen atoms of the network) may release and contribute in conduction with the Ag^+ ions (which surrounded by I^- ions), and this will lead to increase the concentration of mobile Ag^+ ions. It should be mentioned here that the formation of more open glassy structure with increasing AgI content (as mentioned before in thermal analysis results) can facilitate the transport of Ag^+ in the glass. The abnormal trend for the sample with x=0.8, i.e., the decrease in σ_{DC} with the concentration of AgI increasing may be attributed to the formation of AgI crystallites in the glass texture of the sample, as mentioned above.

In order to give information on the type of polarization present in the samples, the AC electrical conductivity (σ_{AC}), dielectric constant (ε'), and dielectric loss (ε'') at temperatures between 303 and 413 K and a frequency range of 10^2–10^6 Hz were studied. The AC conductivity $\sigma_{AC}(\omega)$ was calculated by subtracting the measured DC conductivity (σ_{DC}) from the measured total frequency-dependent conductivity $\sigma_t(\omega)$ such that

$$\sigma_{AC}(\omega) = \sigma_t(\omega) - \sigma_{DC} \quad (5)$$

In Fig. 6a, isotherms of AC conductivity are plotted for the glass with a composition of x=0.5 whereas in Fig. 6b, AC conductivity is presented as a function of inverse temperature at different frequencies for the same glass. The frequency dependence of AC conductivity at a given temperature showed almost two regions [21], where at low-frequency region, the conductivity is slightly dependent on frequency and represents the long-range transport of the ions. It should be noted that the dispersion starts at a higher frequency with temperature increasing. However, at low temperature and frequency, the leveling-off of the conductivity is sufficiently distinct. Other glasses also showed similar behavior. The switch over from the lower frequency region slightly dependent on the frequency-dependent region signs the onset of conductivity relaxation (dispersion), which shifts toward higher frequencies with temperature. The increase of conductivity with temperature is due to the existence of different kinds of inhomogenities in the solids, i.e., a strong frequency dispersion of the conductivity is observed only in disordered solids. The inhomogenities in the solid material may be of microscopic in nature with the distribution of relaxation processes occurring in disordered solids. There are several approaches in the literature to explain this behavior [22–26]. Also, one possible explanation is given by Funke [27].

The variation of conductivity with frequency may be expressed to the well-known power law of AC behavior which

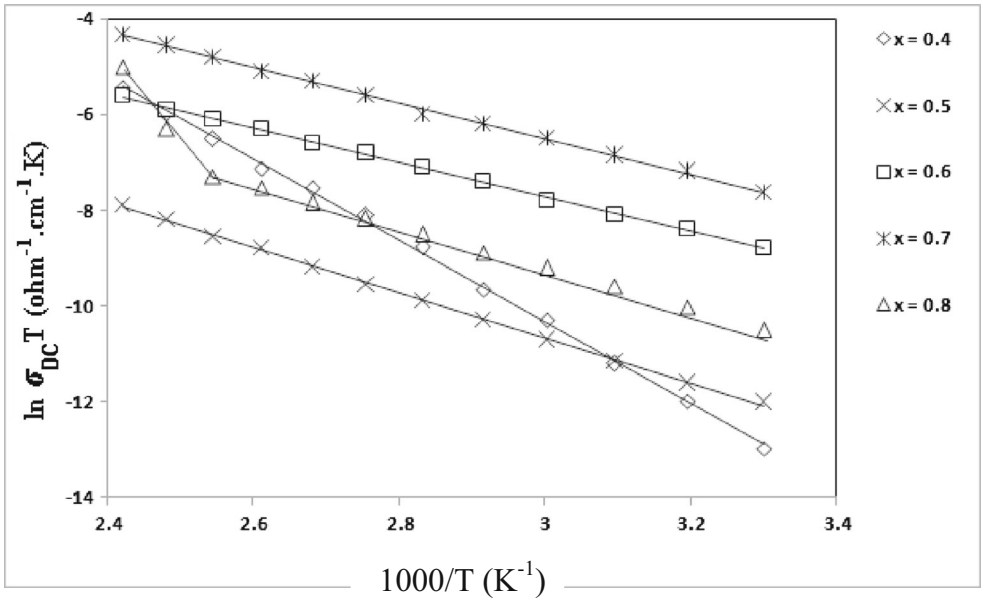

Fig. 5 Temperature dependence of DC conductivity for xAgI – (1-x)[0.67Ag2O-0.33V2O5] glasses, where x = 0.4 , 0.5, 0.6 , 0.7 and 0.8"

indicates a non-random process wherein the ion motion is correlated [28–30] and given by Eq. 6:

$$\sigma_{AC}(\omega) = A\,\omega^{s} \tag{6}$$

where A is a pre-exponential factor that depends on temperature and composition, and s is the dimensionless frequency exponent. The frequency exponent s was calculated from the slope of the log $\sigma_{AC}(\omega)$ versus log ω, which is a straight

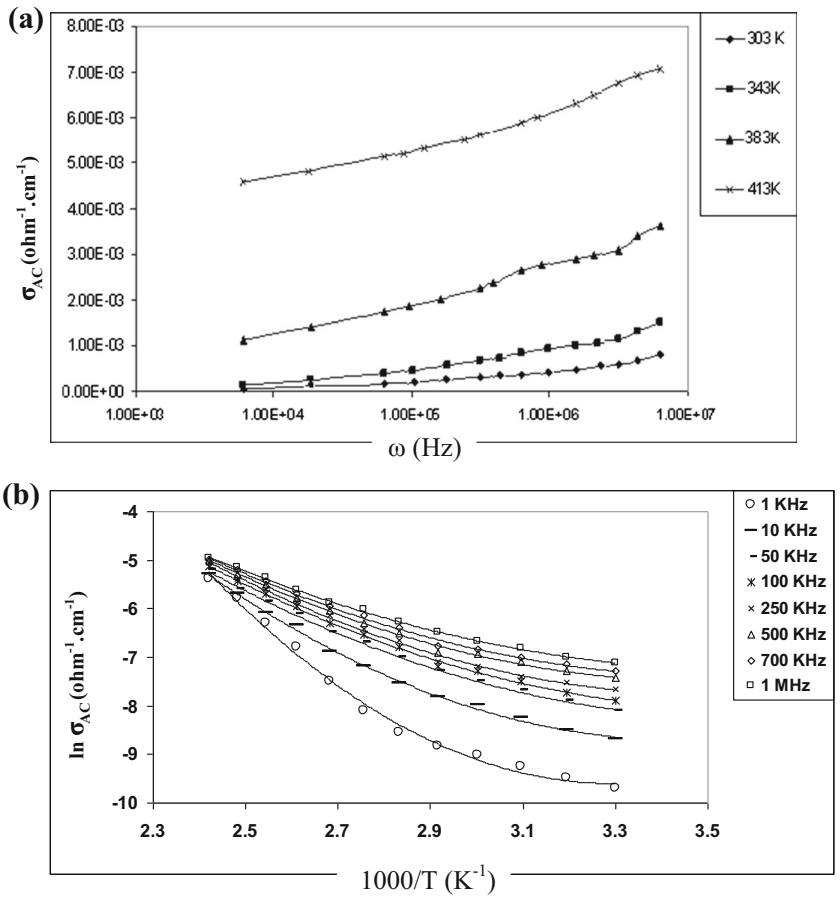

Fig. 6 Effect of temperature and frequency on AC electrical conductivity of $(AgI)_{0.4}[0.67Ag_2O–0.33V_2O_5]_{0.6}$

Table 3 AC conductivity data for the glass system xAgI–(1−x)[0.67Ag_2O–0.33V_2O_5] (x=0.4, 0.5, 0.6, 0.7, and 0.8)

xAgI	Temperature range (K)	E_{AC} (eV)		
		50 KHz	500 KHz	1 MHz
0.4	303–353	0.23	0.20	0.17
	363–413	0.36	0.32	0.31
0.5	303–363	0.19	0.14	0.11
	373–413	0.35	0.33	0.29
0.6	303–363	0.17	0.13	0.10
	373–413	0.32	0.30	0.27
0.7	303–363	0.16	0.13	0.10
	373–413	0.29	0.27	0.25
0.8	303–373	0.19	0.15	0.12
	383–413	0.32	0.26	0.22

line. Since the calculated values of exponent s lie in the range 0.06–0.36, the correlation motion is sub-diffusive and indicates a preference on the part of ions that has hopped away to return to where it started.

From the plots of log σ_{AC} versus $1/T$ (Fig. 6b), we have evaluated the activation energy E_{AC} using Arrhenius law. The results obtained are listed in Table 3. The increase in σ_{AC} with temperature can be also explained on the basis that the temperature rising causes more structure relaxation and releasing more of Ag^+ ions attached to the non-bridging oxygen to become more mobilized. This may be also due to the drift mobility and hopping frequency increasing of charge carriers.

Generally, our results can be also explained according to the unified site relaxation model. This model contains the essentials of both the jump relaxation model [28] and the dynamic structure model [31]. Accordingly, it accounts for the two different kinds of site relaxation introduced in the two models (Coulomb relaxation and network relaxation). The Coulomb relaxation is performed by correlated hops of neighboring ions; it is much faster than any restructuring of the surrounding glassy network which may be necessary to accommodate a mobile ion after a hop. According to the unified site relaxation model, the frequency-independent conductivity (at high temperatures) may be attributed to the long-range transport of mobile silver ions in response to the applied electric field.

The complex permittivity $\varepsilon^*(\omega)$ can be expressed as a complex number: $\varepsilon^*(\omega)=\varepsilon'(\omega)-j\varepsilon''(\omega)$, where $\varepsilon'(\omega)$ and $\varepsilon''(\omega)$ are the real part known as dielectric constant and

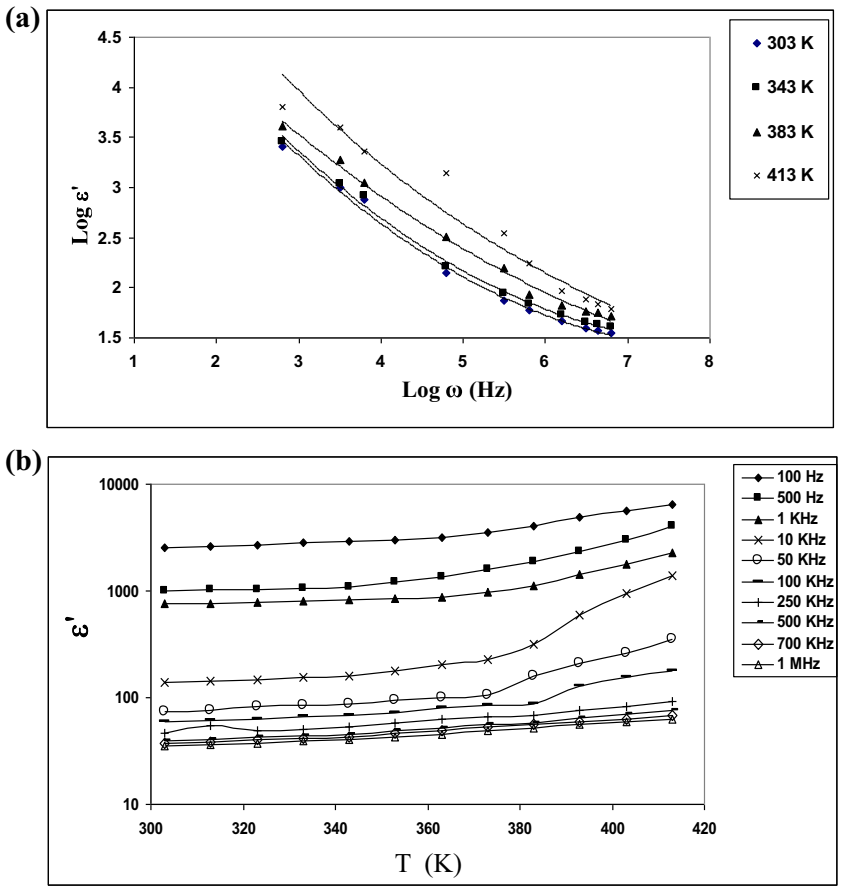

Fig. 7 Effect of temperature and frequency on dielectric constant of $(AgI)_{0.5}[0.67Ag_2O–0.33V_2O_5]_{0.5}$

imaginary part known as dielectric loss of the complex permittivity. It was observed that at each constant temperature and frequency, the dielectric parameters increase with the AgI content in the glass.

The dielectric constant dispersion, $\varepsilon'(\omega)$, at various temperatures for the glass sample with $x=0.5$ is depicted in Fig. 7a, whereas in Fig. 7b, variation of $\varepsilon'(\omega)$ with temperature for the same glass sample is presented. At high frequency, $\varepsilon'(\omega)$ approaches to a constant value, $\varepsilon'_{\infty}(\omega)$, which is probably attributed to a rapid polarization process with no ionic movement contribution (the frequency is too high, and the ions can only oscillate without reaching the sample–electrode interface) [32]. With frequency decreasing, dielectric constant shows a high value, $\varepsilon'_s(\omega)$. This can be attributed to the formation of a thin depletion layer of Ag^+ near the positive electrode together with the interfacial polarization present in the sample [33]. The temperature dependence of ε' (Fig. 7b) shows an increase in ε' with the temperature rising. This is explained on the basis that as the temperature increases, the thermal energy librates more localized dipoles and the field tries to align them in its direction. This occurs either by rotational or orientation motion contributing to an increase in ε'. The variation of dielectric constant with temperature and frequency for all other glasses has demonstrated similar behavior. Interestingly, the dispersion of dielectric loss, ε'', with frequency and temperature is also found to be similar. Typical plot is shown in Fig. 8a, b, for the sample with a composition of $x=0.5$. The high value obtained for dielectric loss is considered to be a contribution mainly from high ionic conductivity and much less from electronic conductivity. Generally, the high ε'' value is a characteristic feature for all high ionic conducting materials [34].

The frequency dependence of ε'' for all investigated samples shows two dispersion regions: a low frequency region below ~10^4 Hz and a high one at more than 10^4 Hz. The low-frequency dispersion of ε'' may be partly due to the intrinsic DC conductivity of the sample. The high frequency dependence, on the other hand, may be attributed due to presence of some clusters such as AgI in the glass matrix. Generally, the decrease in ε'' with frequency can be expressed by the following relation [35]:

$$\varepsilon''(\omega) = A\,\omega^m \tag{7}$$

where $m=(-4kT/W_m)$, W_m being the energy required to liberate a carrier that hops in localized sites. The W_m values are obtained using the least squares fitting of Eq. 7 and given in Table 2. The values of W_m are lower than E_{DC} (the activation energies obtained from DC conductivity data) for all the

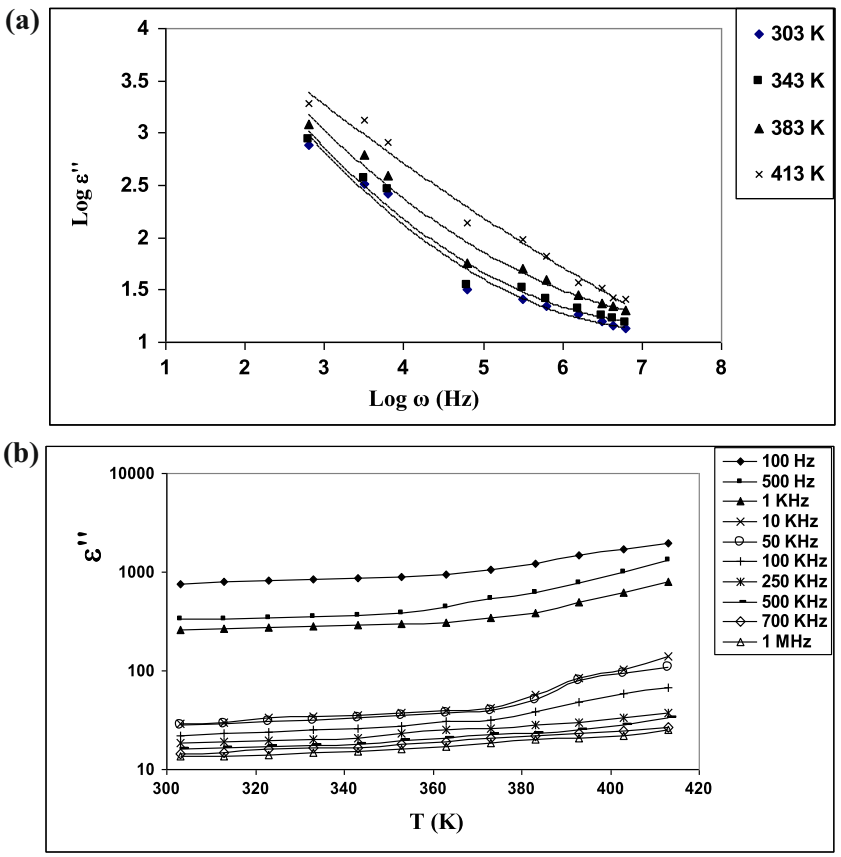

Fig. 8 Effect of temperature and frequency on dielectric loss for $(AgI)_{0.5}[0.67Ag_2O–0.33V_2O_5]_{0.5}$

investigated samples. This can be attributed to the remarkable contribution of the localized electrons of the amorphous matrix in the conduction process. Also, it is noticed that the W_m value for sample with x=0.8 is higher than that of other ones. This can be attributed to the presence of larger amounts of crystallite AgI in addition to the structure rigidity and less door ways for the glassy system [36].

Conclusions

Ternary ionic conducting glass system, xAgI–$(1-x)[0.67Ag_2O–0.33V_2O_5]$, where x=0.4, 0.5, 0.6, 0.7, and 0.8, were prepared using melt quenching technique. The shifts of FTIR bands and glass transition temperature, T_g, with silver iodide concentration increasing refer to the influence of AgI in the formation of more opened network structure. The higher the amount of AgI, the lower the cross-link density and the lower T_g value, except for the sample with a composition of x=0.8. The electrical properties of the studied glasses change with concentration of silver iodide. The analysis of the conductivity results for all glass compositions showed a mixed ionic–electronic conduction with high ionic conductivity value for the sample with x=0.7. Each of ionic transfer number and DC conductivity (σ_{DC}) for vanadate system increases, at room temperature, in the order of σ_{DC} (x=0.7) > σ_{DC} (x=0.6) > σ_{DC} (x=0.8) > σ_{DC} (x=0.5) > σ_{DC} (x=0.4). The correlated barrier-hopping (CBH) model is found to be appropriate for explaining the AC conductivity as a function of frequency and temperature.

References

1. Varsamis CP, Kamitsos EI, Chryssikos GD (2000) Solid State Ionics 136–137:1031
2. Bhattacharya S, Ghosh A (2003) Solid State Ionics 161:61
3. Srilatha K, Sambasiva Rao K, Gandhi Y, Ravikumar V, Veeraiah N (2010) J Alloy Compd 507(2):391
4. Foltyn M, Wasiucionek M, Garbarczyk J, Nowiński JL (2005) Solid State Ionics 176(25–28):2137
5. El-Shaarawy MG, Bayoumy WA (2004) J Phys Soc of Japan 77:207
6. Murawski SL, Barczyński RJ (2005) Solid State Ionics 176(25–28): 2145
7. Garbarczyk JE, Wasiucionek M, Machowski P, Jakubowsk W (1999) Solid State Ionics 119(1–4):9
8. Wasiucionek M, Garbarczyk JE, Wn trzewski B, Machowski P, Jakubowski W (1996) Solid State Ionics 92(1–2):15
9. Machowski P, Garbarczyk JE, Wasiucionek M (2003) Solid State Ionics 157(1–4):281
10. Laplume J (1955) Onde Electr 35:355
11. Agrawal RC, Kumar R (1994) J Phys D Appl Phys 27:2432
12. Padmasree KP, Kanchan DK, Panchal HR, Awasthi AM, Bharadwaj S (2005) Solid State Commun 136:102
13. Dimitriev Y, Dimitrov V, Arnaudov M, Topalov D (1983) J Non Cryst Sol 57:147
14. Chiodelli G, Magistris A, Villa M, Bjorkstam JL (1982) J Non Cryst Sol 51:143
15. Exarhos GJ, Risen WM (1972) Solid State Commun 11:755
16. Panchal HR, Kanchan DR, Somayjulu DRS (1969) Mater Sci Forum 223–224:301
17. Jayasinghe GDLK, Diassanayake MAKL, Bandaranayake PWSK, Souquet JL, Foscallo D (1999) Solid State Ionics 121:19
18. Sekhon SS, Chandra S (1999) J Mater Sci Lett 18:635
19. Chandra S (1981) "Superionic solids". North-Holland Publ.Co, Amsterdam
20. Minami T (1983) J Non Cryst Sol 56:15
21. Jonscher AK (1983) Dielectric relaxation in solids. Chelsea Dielectric Press, London
22. Baranovskii SD, Cordes H (1999) J Chem Phys 111:7546
23. Vogel M (2004) Phys Rev B 70:094302
24. Garcia-Belmonte G, Bisquert J (2004) J Non Cryst Solids 337:272
25. Dyre JC, Schoder TB (2000) Rev Mod Phys 72:873
26. Bale S, Rahman S (2012) Mat Res Bull 47:1153
27. Funke K (1993) Prog Solid State Chem 22:111
28. Pant M, Kanchan DK, Sharma P, Jayswal MS (2008) Mat Sci Eng 149(1):18
29. Sidebottom DL (1999) Phys Rev Lett 82:3653
30. Schroder TB, Dyre JC (2000) Phys Rev Lett 84:310
31. Bunde A, Ingram MD, Maass P (1994) J Non Cryst Sol 17:1222
32. Sidebottom L, Roling B, Funke K (2000) Phys Rev B 63:024301
33. Amderson S (1955) J Am Ceram Soc 38:370
34. Laskar AL, Chandra S (1989) "Superionic solids and solid electrolytes": recent trends. Academic, New York
35. Giuntini JC, Zanchetta JV, Jullien D, Eholie R, Houenou P (1981) J Non-Cryst Solids 45:57
36. Soliman SM (1998) Ph.D. Thesis, Faculty of Science, Benha University, Benha, Egypt